Fluid simulations of mirror constraints on proton temperature anisotropy in solar wind turbulence

D. Laveder, L. Marradi, T. Passot, P.L. Sulem

Fluid simulations of mirror constraints on proton temperature anisotropy in solar wind turbulence

D. Laveder,[1] L. Marradi,[1] T. Passot,[1] and P. L. Sulem[1]

Received 13 July 2011; revised 12 August 2011; accepted 13 August 2011; published 10 September 2011.

[1] Non-resonant ion perpendicular heating by low-frequency kinetic Alfvén wave turbulence, together with the constraining effect of the mirror instability on the developing temperature anisotropy observed in the solar wind, are simulated for the first time in a self-consistent way using a fluid model retaining low-frequency kinetic effects. This model which does not include solar wind expansion, concentrates on the influence of small-scale turbulence. It provides a sufficiently refined description of Landau damping and finite Larmor corrections to accurately capture the transverse dynamics at sub-ionic scales, including the self-regulating influence of the developing mirror modes. A fit of the simulation results with the usual mirror-instability threshold is obtained, reproducing the frontier of the slow solar wind WIND/SWE data in the ($T_{\perp i}/T_{\|i}$, $\beta_{\|i}$) diagram. The quality of the fit is improved in the presence of a small amount of collisions, which suggests that the deviations from bi-Maxwellianity in the slow solar wind are weak enough not to significantly affect the mirror threshold. **Citation:** Laveder, D., L. Marradi, T. Passot, and P. L. Sulem (2011), Fluid simulations of mirror constraints on proton temperature anisotropy in solar wind turbulence, *Geophys. Res. Lett.*, *38*, L17108, doi:10.1029/2011GL048874.

1. Introduction

[2] Special interest has recently been paid to the temperature anisotropy that develops in the solar wind under the effect of expansion, turbulence and field-particle interactions. Analysis of the proton temperatures and of the parameter $\beta_{\|i}$ measured in the slow solar wind by the WIND/SWE mission suggests that the proton temperature anisotropy is constrained by oblique micro-instabilities, either mirror or firehose, depending on the dominance of the perpendicular or parallel temperature respectively, although the linear theory in the case of a proton-electron plasma predicts a preponderance of the proton cyclotron and of the parallel firehose instabilities. This apparent discrepancy could be due to the presence of minor ions in the solar wind that may stabilize the ion cyclotron waves sufficiently for the mirror instability to become the dominant effect [*Price et al.*, 1986].

[3] The role of mirror and firehose instabilities is exemplified in Figure 1 of *Hellinger et al.* [2006] that shows a color-scale plot of the relative frequency of ($\beta_{\|p}$, $T_{\perp p}/T_{\|p}$). It appears that the data do not extend significantly beyond the contour of a near-zero maximum growth rate for the above instabilities as estimated for a plasma with a bi-Maxwellian ion distribution function with the corresponding temperatures and isothermal electrons. Adding 5% of alpha particle does not sizeably affect these contours, but shifts the threshold of the ion cyclotron instability, especially at small $\beta_{\|i}$ [*Matteini et al.*, 2011]. It is noticeable in this context that observational data reach the mirror threshold for values of $\beta_{\|i}$ as small as 0.1. In the fast wind, where the collisions are significantly weaker, the agreement does not seem so accurate [*Hellinger et al.*, 2006; *Matteini et al.*, 2007]. A similar conclusion is reached by *Bale et al.* [2009] who analyzed 10^6 independent measurements of gyroscale magnetic fluctuations in the solar wind, from experiments on the WIND spacecraft. An additional result is that the amplitude of these fluctuations are enhanced when the plasma is close to the instability thresholds. Furthermore, the relative importance of the parallel magnetic fluctuations as measured by the "magnetic compressibility" $\delta b_{\|}^2/(\delta b_{\|}^2 + |\delta b_{\perp}|^2)$ is greatly increased for $\beta_{\|i} \gtrsim 1$ close to the mirror threshold.

[4] We concentrate here on the case where perpendicular proton heating is dominant, a regime whose origin is still debated. A process based on the coupling of fast waves to proton cyclotron Bernstein mode in a small beta plasma such as the solar corona was considered by *Markovskii et al.* [2010] who performed hybrid simulations for $\beta_i = 0.02$. At larger distance from the sun, where the turbulent fluctuations are dominated by quasi-transverse kinetic Alfvén waves, non-resonant mechanisms are to be considered [*Bourouaine et al.*, 2008]. Recent test-particle simulations showing perpendicular ion heating by prescribed low-frequency Alfvén-waves with random phases are reported by *Chandran et al.* [2010]. A fully nonlinear hybrid simulation in the free decay regime in two space dimensions, with isothermal electrons and initial purely transverse magnetic perturbations in the form of the so called Orszag-Tang vortex, shows a weak increase of the mean ion temperature perpendicular to the guide field [*Parashar et al.*, 2009].

[5] The present paper addresses the quasi-transverse dynamics of a magnetized proton-electron plasma, focusing on the role played by the mirror instability. The system is subject to a random driving in a way as to mimic the energy injection from the end of the solar-wind Alfvén-wave cascade that is believed to act preferentially in directions quasi-perpendicular to the ambient field. Numerical simulations are presented, based on a "FLR-Landau fluid" model that involves a closure of the fluid hierarchy at the level of the fourth-rank moment, retaining low-frequency kinetic effects such as Landau damping and ion finite Larmor radius (FLR) corrections, as needed to address the mirror instability [*Passot and Sulem*, 2007]. We assume that space variations only take place along a direction making a prescribed angle with the ambient magnetic field and present for the first time, fully nonlinear simulations of regimes displaying dominant ion transverse heating, where mirror instability develops and

[1]Université de Nice-Sophia Antipolis, CNRS, Observatoire de la Côte d'Azur, Nice, France.

0094-8276/11/2011GL048874

constrains the temperature anisotropy to remain close to threshold. It turns out that retaining a weak level of collisions ensures an excellent agreement with observations in the slow solar wind.

2. The FLR-Landau Fluid Model

[6] It is well known that the usual fluid descriptions are poorly adapted to the solar wind at the ionic and sub-ionic scales. Landau resonance has indeed a main effect in damping magnetosonic waves and depleting the longitudinal dynamics (P. Hunana et al., Reduction of compressibility and parallel transfer by Landau damping in turbulent magnetized plasmas, submitted to *The Astrophysical Journal*, 2011), while an accurate description of the FLR corrections is needed to quench at small scales the microinstabilities driven by temperature anisotropy. A closure relation retaining linear Landau damping consistent with the linear kinetic theory was implemented in the case of large-scale MHD by *Snyder et al.* [1997], for the moment hierarchy derived from the drift-kinetic equation, leading to the so-called Landau fluid model. A generalization (hereafter referred to as the FLR-Landau fluid model) which retains quasi-transverse sub-ionic scales is presented by *Passot and Sulem* [2007]. In contrast with the gyrokinetic description which reproduces the reduced MHD in the large-scale limit [*Schekochihin et al.*, 2009], Landau fluids reduce to full MHD as they retain fast waves that are accurately described up to the ion gyroscale. Nevertheless, by construction, none of these two approaches can retain fast dynamical processes such as the ion cyclotron resonance.

[7] The FLR-Landau fluid model is constructed by deriving from the Vlasov-Maxwell system a moment hierarchy which starts with equations for the plasma density ρ and for the ion velocity u where, for the sake of simplicity, the electric field is expressed by the generalized Ohm's law, obtained after neglecting the electron inertia. The ion pressure tensor includes both gyrotropic and non-gyrotropic contributions $\mathbf{p}_i = p_{\perp i}\mathbf{I} + (p_{\|i} - p_{\perp i})\boldsymbol{\tau} + \boldsymbol{\Pi}_i$ with $\tau = \widehat{b} \otimes \widehat{b}$ ($\widehat{b} = b/|b|$ indicating the direction of the local magnetic field), while in the electron pressure tensor $\mathbf{p}_e = p_{\perp e}\mathbf{I} + (p_{\|e} - p_{\perp e})\, \widehat{b} \otimes \widehat{b}$, the non-gyrotropic (or FLR for finite Larmor radius) corrections are neglected. The equations governing the gyrotropic pressures and heat fluxes $q_{\perp r}$ and $q_{\|r}$ of each particle species r, are given by *Passot and Sulem* [2007]. These equations involve the gyrotropic fourth-rank velocity cumulants and also contributions originating from the non-gyrotropic pressures, heat fluxes and fourth order moments which are all estimated from the low-frequency linear kinetic theory by combining the kinetic expressions of the various quantities in a way that minimizes the occurrence of the plasma dispersion relation. The latter is otherwise replaced by Padé approximants in a way that finally leads to local-in-time equations, suitable for an initial value problem. Explicit expressions of the various contributions in the case where the space variations only take place in a direction making a prescribed angle with the ambient field are given by *Borgogno et al.* [2007] and *Camporeale et al.* [2010]. Involving heat fluxes and fourth-rank cumulants, the present model is able to describe regimes associated with moderate departures from bi-Maxwellian distribution functions.

[8] Detailed comparison with the kinetic theory demonstrates that the FLR-Landau fluid model correctly reproduces the mirror instability and its quenching at small scales. It also accurately reproduces the frequency and the damping rate of (quasi-transverse) kinetic Alfvén waves, while in moderately oblique directions, the accuracy is limited by the presence of resonances. It furthermore preserves the conservation of the mean energy $\langle(1/2)\ (\rho|u|^2 + |b|^2) + (\beta_0/2)\ (p_{\perp i} + p_{\perp e} + (p_{\|i}/2 + p_{\|e}/2))\rangle$, where β_0 is the initial parallel beta of the ions, that enters the formula when using the units defined at the end of this section. It is noticeable that due to the Landau damping and the dispersive effects introduced by the Hall term and the FLR corrections, accurate numerical integrations of the above equations can be performed without any additional regularizing or filtering process, in spite of the extremely low numerical dissipation (typically 10^{-11} smaller than the energy injection rate). This situation originates from the exponential decay of the spectra of the various fields, except during brief events that occur in the long-time dynamics and could correspond to Alfvén resonances [*Bellan*, 1994, and references therein].

[9] As discussed below, it appears to be of interest to retain the effect of weak collisions. A simple approach is the Bhatnagar-Gross-Krook (BGK) model [*Gross and Krook*, 1956; *Bhatnagar*, 1962] that consists in adding a term $-\sum_\beta \nu_{\alpha\beta}\, \frac{\rho}{\rho_0}\, (f_\alpha - F_{\alpha\beta})$ in the right hand side of the Vlasov equation for the distribution function f_α of species α (ions or electrons). The coefficients $\nu_{\alpha\beta}$ are the collision frequencies at equilibrium of the β species on the α species in the frame of the latter, and the subscript zero refers to the (uniform) initial condition of the number or mass density. As well known, they are related by $\nu_{ii} = (\frac{m_e}{m_i})^{1/2}\nu_{ee}$, $\nu_{ie} = \frac{m_e}{m_i}\nu_{ee}$ and $\nu_{ei} = \nu_{ee}$. Here, following *Snyder et al.* [1997], we choose (n denoting the number density) $F_{\alpha\beta} = \frac{n m_\alpha^{3/2}}{(2\pi)^{3/2} T_\alpha^{3/2}} \exp(-\frac{m_\alpha |v-u_\beta|^2}{2T_\alpha})$ with $T_\alpha = \frac{1}{3}\ (T_{\|\alpha} + 2T_{\perp\alpha})$. We assume that the collision frequencies $\nu_{\alpha\beta}\frac{\rho}{\rho_0}$ are proportional to the instantaneous number density (a condition necessary to ensure energy conservation), but neglect their temperature dependence for the sake of simplicity. The limitations of this model are well known [*Livi and Marsh*, 1986], but its use appears convenient within a fluid approach, while obtaining analytic expressions for the moments of the Coulomb operator does not seem possible. Generalized BGK models where the collision frequencies decay with the particle velocities are discussed by *Livi and Marsh* [1986], but do not exactly preserve the conservation laws.

[10] The collision model used in this letter is suitable to describe the thermalization of the electron and ion populations but not the (significantly slower) approach to an equilibrium associated with equal temperatures and hydrodynamic velocities for the two species [*Green*, 1973]. It induces additional terms in the equations for the gyrotropic pressures and heat fluxes for each of the particle species, that are similar to those given by *Snyder et al.* [1997], up to supplementary contributions which involve the current j, and also a term of magnetic diffusion in the equation for the magnetic induction. Although needed to ensure the conservation of the total energy, these terms (associated with Joule heating) are in fact negligible. Furthermore, a purely linear damping $-(\nu_{rr} + \nu_{ie})\frac{\rho}{\rho_0}\widetilde{r}_{\perp\|r}$ is added in the equation for $\widetilde{r}_{\|\perp r}$ which is the only fourth-rank cumulant obeying a dynamical closure equation.

[11] The numerical simulations of the FLR-Landau-fluid equations presented here were performed with initially iso-

tropic and equal temperatures of the ions and the electrons, for various values of β_0. The injection of energy at the end of the solar-wind Alfvén-wave cascade is simulated by a white-noise-in-time driving supplemented in the equation for the velocity component perpendicular to the plane defined by the ambient field and the direction of propagation. The forcing acts at prescribed scales, large compared to the ion Larmor radius, with fixed amplitudes and phases randomly chosen at each time step. It is only active when the density of the sum of the kinetic and magnetic fluctuation energies $E_M = \frac{1}{2}\langle\rho|u|^2\rangle + \frac{1}{2}\langle|b - B_0\,\widehat{e}_z|^2\rangle$ remains below a fixed threshold, in order to maintain a prescribed level of turbulence. Here, the brackets denote average on the space domain. Driving the velocity field rather than the magnetic field has the advantage of not affecting directly the space averaged magnetic moment per unit mass $\langle\frac{p_{\perp i}}{|b|}\rangle$ that obeys

$$\frac{d}{dt}\left\langle\frac{p_{\perp i}}{|b|}\right\rangle = \left\langle\frac{p_{\perp i}}{|b|^2}\widehat{b}\cdot\left[\nabla\times\frac{m_i c}{\rho e}\left(\frac{j\times b}{c} - \nabla\cdot\mathbf{p}_e\right)\right]\right\rangle + \left\langle\frac{1}{2|b|^2}S^{\perp}_{\perp i}\cdot\nabla|b|\right\rangle + \left\langle\frac{1}{2|b|}\left[\mathrm{tr}(\mathbf{\Pi}_i\cdot\nabla u_i\right)^s - (\mathbf{\Pi}_i\cdot\nabla u_i)^s : \boldsymbol{\tau} + \mathbf{\Pi}_i : \frac{d\boldsymbol{\tau}}{dt}\right\rangle\Bigg], \quad (1)$$

where the variations only originate from the Hall effect, the electron pressure gradient and the FLR contributions $\mathbf{\Pi}_i$ and $S^{\perp}_{\perp i}$ to the ion pressure and perpendicular heat flux. The superscript s indicates that the tensor is symmetrized. Note that in the gyrokinetic theory that deals with the distribution function of the gyrocenters rather than with that of the particles, the corresponding magnetic moment is, by construction, conserved [*Brizard and Hahm*, 2007], but differs from the magnetic moment of the fluid theory.

[12] After rewriting the FLR-Landau fluid equations using units derived from the magnitude of the ambient field, the Alfvén velocity, the ion inertial length d_i, together with the (uniform) initial density and parallel ion pressure, we integrate them using a spectral method with an effective resolution of 256 grid points (after a partial dealiasing where the nonlinear terms are evaluated with twice the number of Fourier modes), in a computational domain of size $L = 16\pi \times (\beta_0/0.6)^{1/2}$, along a direction making an angle of 80° with the ambient magnetic field. As a consequence, the maximal wavenumber satisfies $k_{\max}\, r_L = 12.4$ where $r_L = d_i\sqrt{\beta_0}$ is the initial ion Larmor radius. This choice of the domain size is aimed to ensure a fixed ratio between the driving scales (peaked about $L/4$ in all the simulations) and the ion Larmor radius when changing β_0. The time stepping is performed using a third order Runge-Kutta scheme with a time step Δt ranging between 10^{-4} and 10^{-3} depending on the conditions.

3. Development of Temperature Anisotropy and Mirror Constraining Effect

[13] In agreement with the test particle simulations of *Chandran et al.* [2010], we observe that when the turbulence energy is large enough at scales comparable to the ion Larmor radius, the ions are heated predominantly in the perpendicular direction. The rate of variation of the perpendicular temperature is larger when the value β_0 of the initial beta (here taken equal for the ions and the electrons) is smaller. Nevertheless, when considering the time variation of the contribution $\beta_0\ \langle p_\perp\rangle$ to the internal energy, the influence of β_0 is negligible. The heating properties are in contrast strongly dependent on the typical scales and amplitude of the injected waves. Indeed, inspection of equation (1) shows that the breaking of the magnetic moment invariance (that is directly related to perpendicular temperature variation) is mostly due to the FLR contributions which are only significant at ionic scales. The heating process results from a continuous transformation of the energy carried by transverse waves into heat, rather than from intermittent events like shocks. A detailed understanding of such a non-resonant ion heating actually requires an analysis of microscopic processes which is beyond the scope of the present letter.

[14] In our simulations, energy injection takes place near the wavenumber $k_{\rm inj} = 4 \times 2\pi/L$, corresponding to $k_{\rm inj}\ r_L = 0.39$. We first report on the case of a collisionless plasma with $\beta_0 = 0.6$. Although in a fully kinetic three-dimensional simulation in the absence of minor ions, the ion cyclotron instability could play a role at such a beta, we concentrate here on the mirror instability that, when it takes place, displays robust properties qualitatively independent of the value of beta. The motivation for using a relatively small beta in the present simulations is to ensure that the initial conditions, that have isotropic temperatures, be far enough from the mirror threshold. In this simulation, we chose to maintain the root mean square of the transverse magnetic field fluctuations of the order of 0.12 times the magnitude of the ambient field, corresponding to typical maxima of the normalized magnetic field fluctuations of the order of 0.26. This regime is obtained by driving the system only when the sum of the kinetic and magnetic fluctuations in the full domain is smaller than 0.8 (in code units), which corresponds to an energy density threshold $E_M = 0.0159$. Analysis of CLUSTER data in the solar wind for the observation period whose parameters are reported in Table I (2nd column) of *Alexandrova et al.* [2009] indicates that the values retained for the simulations are only weakly overestimated, typically by a factor 2 (O. Alexandrova, private communication, 2011), a choice motivated by computational constraints. Some lower turbulence levels are considered in the following.

[15] Figure 1 (top) shows the time evolution of the space-averaged temperatures. The ion perpendicular and the electron parallel temperatures always increase, the latter at a significantly smaller rate, while the perpendicular electron temperature stays almost constant. Differently, the parallel ion temperature decreases at early times (until $t \approx 5000$), before growing at a rate slower than the perpendicular one. Detailed inspection of the contributions of the different terms in the pressure equations shows that the dominant effect at the origin of the initial ion perpendicular heating and parallel cooling is the work of the force due to the non-gyrotropic pressure $\mathbf{\Pi}_i$. The resulting growth of the ion temperature anisotropy proceeds up to the moment when the mirror instability threshold is reached. The onset of the mirror structure near this time is clearly seen in Figure 1 (middle) that displays a (x, t) color plot of the longitudinal magnetic fluctuations b_z, together with typical snapshots of this field. The formation of structures that, most of the time, are quasi-static is conspicuous, while the transverse velocity component u_x (that is dominantly associated with fast waves) evolves rapidly (not shown). Figure 1 (bottom) also shows

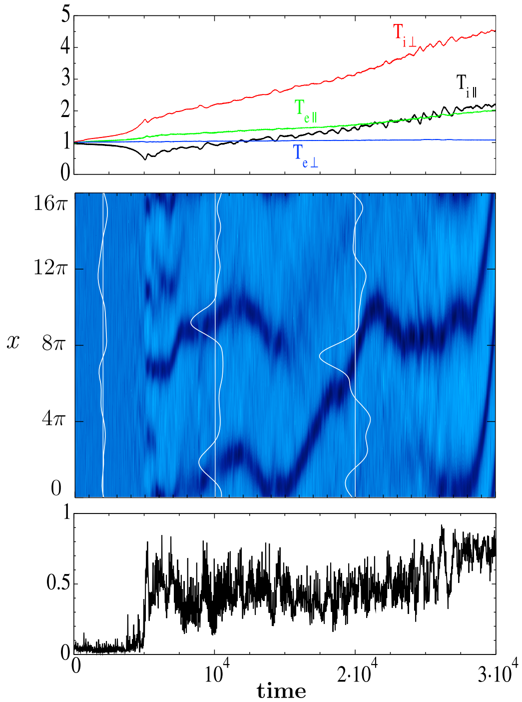

Figure 1. (top) Time evolution of the ion and electron temperatures in the case β_0 = 0.6 and $E_M = E_{M0}$; (middle) color plot of the corresponding longitudinal magnetic fluctuations in the (*t,x*)-plane, together snapshots of the magnetic component b_z (in arbitrary units) displaying mirror structures; (bottom) time evolution of the magnetic compressibility.

the time evolution of the magnetic compressibility $(b_z - B_0)^2/((b_z - B_0)^2 + |b_\perp|^2)$ which displays a sharp increase when the mirror structures start forming. The mirror instability constrains the temperature anisotropy by the fact that the formation of mirror structures tends to decrease the ratio $T_{\perp i}/T_{\|i}$, as seen for example in Figure 3 of *Borgogno et al.* [2007]. The instability thus acts to maintain the system in a regime characterized by a relatively small value of the distance Γ to the instability threshold that, for bi-Maxwellian distribution functions of the ions and the electrons, is given by [*Pantellini and Schwartz*, 1995; *Pokhotelov et al.*, 2000; *Hellinger*, 2007]

$$\Gamma = \frac{T_{\perp i}}{T_{\|i}} - 1 - \frac{1}{\beta_{\perp i}} + \frac{T_{\perp e}}{T_{\perp i}}\left(\frac{T_{\perp e}}{T_{\|e}} - 1\right) - \frac{\left(\frac{T_{\perp i}}{T_{\|i}} + \frac{T_{\perp e}}{T_{\|e}}\right)^2}{2\left(\frac{T_{\perp i}}{T_{\|i}} + \frac{T_{\perp i}}{T_{\|e}}\right)}, \quad (2)$$

where all the temperatures and beta parameters are here to be viewed as instantaneous space-averaged values.

[16] Figure 2 (left) shows the time evolution of the quantity Γ for the simulation described above (β_0 = 0.6, black line), and also with β_0 = 0.3 (green line) and β_0 = 1.2 (red line), the value of $k_{\mathrm{inj}} r_L$ being kept constant. In all the cases, Γ remains confined to a relatively small value depending on the parameters, and displays oscillations reflecting the continuous formation and disruption of mirror structures. The fact that Γ oscillates about a positive value appears to be associated with the existence of non-zero spatial means for the heat fluxes and fourth-rank velocity cumulants that develop during the simulations and are the signatures of deviations from bi-Maxwellian distributions functions for the ions and the electrons. It was indeed numerically checked that for an equilibrium state including non-zero fourth-rank cumulants, the value of the parameter Γ given by equation (2) is positive at threshold. Similarly, including non-zero equilibrium heat fluxes induces a motion of the mirror structures. This effect was clearly identified in the conditions of Figure 1 (middle). It is noticeable that the oscillations in Figure 2 (left) are stronger when β_0 is smaller, as the formation of mirror structures involves a transfer of energy from the internal to the magnetic part, and a corresponding variation of the total temperature which is inversely proportional to β. Another effect of decreasing β_0 is an enhanced magnetosonic activity, which is associated with a larger mean square value of the component u_x and a larger parallel heating rate of the electrons by Landau damping (not shown).

[17] Figure 2 (middle) shows, for β_0 = 0.6, the influence on the time evolution of the parameter Γ, of the level of Alfvénic-like turbulence, by changing the energy threshold $E_M = E_{M0}$ (black line), $E_{M0}/4$ (red line) and $E_{M0}/16$ (green line). We note that, as E_M is reduced, the time needed to reach the mirror threshold increases, consistent with the observation that both the perpendicular heating and parallel

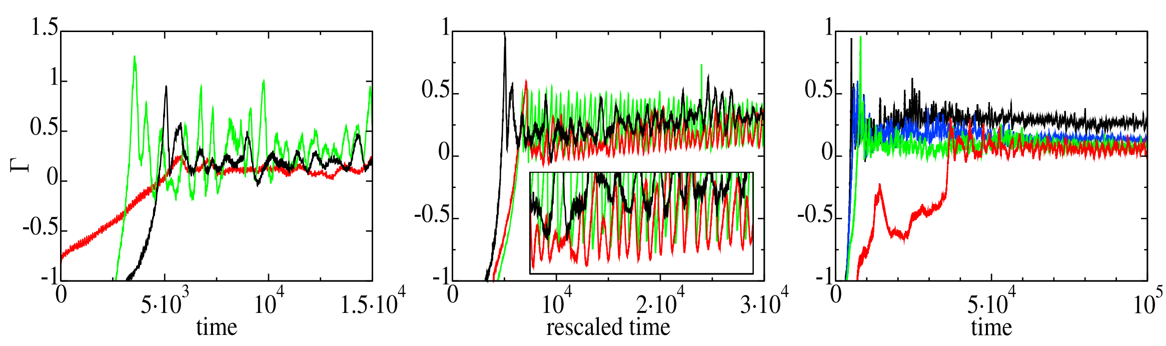

Figure 2. Time evolution of Γ in various regimes. (left) For $E_M = E_{M0}$, ν_{ie} = 0 and β_0 = 0.6 (black), 0.3 (green) 1.2 (red); (middle) for β_0 = 0.6, ν_{ie} = 0 and $E_M = E_{M0}$ (black), $E_M = E_{M0}/4$ (red), $E_M = E_{M0}/16$ (green), the insert corresponding to a zoom between t = 13000 and t = 23000; (right) β_0 = 0.6, $E_M = E_{M0}$ and ν_{ie} = 0 (black), $\nu_{ie} = 6.25 \times 10^{-7}$ (blue), $\nu_{ie} = 2.5 \times 10^{-6}$ (green), $\nu_{ie} = 10^{-5}$ (red).

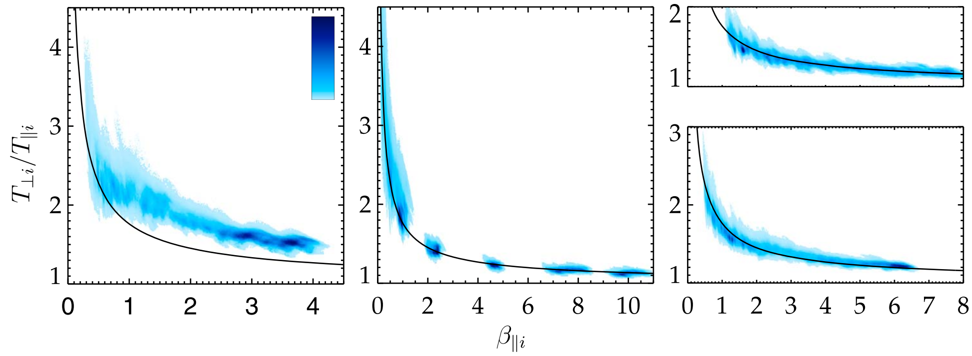

Figure 3. Distribution of the results of numerical data in the ($T_{\perp i}/T_{\parallel i}$, $\beta_{\parallel i}$) plane. (left) simulation with β_0 = 0.6 and E_M = E_{M0} up to $t = 10^5$; (middle) collection of several runs with fixed $E_M = E_{M0}$ (see text); (right) simulations with β_0 = 0.6 and $E_M = E_{M0}$ in the presence of collisions with frequencies (top) $\nu_{ie} = 10^{-5}$ and (bottom) $\nu_{ie} = 0.25 \times 10^{-5}$. Such values are slightly larger that those encountered in the solar wind but by no more than a factor 10 (O. Alexandrova, private communication, 2011). The solid line corresponds to the instability threshold as evaluated in observational publications (see beginning of Section 4).

cooling rates scale almost linearly with the energy of the field fluctuations. Comparison between the black and red lines shows a decrease of the typical magnitude of the parameter Γ (that is evaluated under the assumption of bi-Maxwellian ions and electrons). Indeed, a decrease of E_M reduces the departure from the bi-Maxwellian statistics, as conspicuous when considering the magnitude of the space-averaged cumulant $\langle \tilde{r}_{\parallel\perp} \rangle$ (not shown). When the energy is further reduced from the red to the green lines, $\langle \tilde{r}_{\parallel\perp} \rangle$ does not further decrease, and the minima of the green line are thus not lower than those of the red one (see the insert within Figure 2 (middle), corresponding to a zoom between t = 13000 and t = 23000). The oscillations of the green curve nevertheless have a larger amplitude. Indeed, during the development of the mirror instability, a given amount of thermal energy is transferred to the magnetic form, which in the low-energy case easily leads to an arrest of the external driving. The system then undergoes a cyclic evolution in which mirror structures grow, reduce the temperature anisotropy and almost disappear. Such complete oscillations take place in the conditions of the green line, while the black line corresponds to a regime of persistent mirror structures. The red line is associated with a somewhat intermediate state.

[18] The following interpretation can be given for the persistence of the structures. When the turbulence level is high enough, the amount of energy going into heat during a mirror cycle is larger than the energy of the mirror structure itself, in such a way that the system is almost continuously fed by the external driving. As a consequence, temperature anisotropy is maintained by the turbulence, which enforces the presence of quasi-persistent mirror structures and makes oscillations in Γ less pronounced. Note that as time elapses Γ slowly drifts toward higher values, a tendency associated with the continuous growth of $\langle \tilde{r}_{\parallel\perp} \rangle$. This connection is clearly pointed out by artificially maintaining this latter quantity to zero, which results in suppressing this drift almost completely.

[19] The role of the deviation from Maxwellianity can also be studied by retaining the influence of weak collisions, that are expected to reduce not only the temperature anisotropy but also the magnitude of the high-rank moments. We consider simulations with β_0 = 0.6, an energy threshold E_M = E_{M0}. Figure 2 (right) shows the evolution of the parameter Γ up to $t = 10^5$ inverse ion gyrofrequencies, either in the absence of collisions (black curve) or with $\nu_{ie} = 6.25 \times 10^{-7}$ (blue line), $\nu_{ie} = 2.5 \times 10^{-6}$ (green line) and $\nu_{ie} = 10^{-5}$ (red line), corresponding to $\nu_{ii} = 2.68 \times 10^{-5}$, 1.1×10^{-4} and 4.3×10^{-4} respectively, values that are consistent with the solar wind conditions [*Matteini et al.*, 2011, Figure 4; O. Alexandrova, private communication, 2011], and for which the resistive heating turns out to be very weak compared with the injected energy. Using a turbulence level and collision frequencies in slight excess relatively to realistic values has the advantage of fastening the numerical integration.

[20] The presence of collisions delays the onset of the mirror instability, as they oppose to the development of temperature anisotropy (the early decay of the ion parallel temperature is in particular suppressed). Collisions tend to make the parameter Γ significantly closer to zero and prevent any long-time drift, this effect being progressively suppressed as the collision frequency is lowered. This fact is consistent with the significant reduction of the observed average heat fluxes and fourth-order cumulants relatively to the non-collisional case, especially for the electron species (not shown). It is interesting to note that while the electron temperatures are now isotropic (as in the thermal-core electron population in the solar wind [*Štverák et al.*, 2008]), this isotropization does not seem to have a crucial effect on the parameter Γ. This point was tested by performing simulations where the effect of collisions on the high-order moments is artificially suppressed. Even though electron temperatures become isotropic, deviations from bi-Maxwellianity remain significant and Γ does not get closer to zero.

4. Comparison With Solar-Wind Observations

[21] The results of the FLR-Landau fluid simulations can usefully be reformulated in terms of the evolution of the system in the plane ($\beta_{\parallel i}$, $T_{\perp i}/T_{\parallel i}$) considered when analyzing solar wind data [*Hellinger et al.*, 2006; *Matteini et al.*, 2007; *Bale et al.*, 2009]. It turns out that a large majority of the observational measurements in the case of a dominant perpendicular ion temperature are limited from above by the curve $T_{\perp i}/T_{\parallel i} - 1 - 0.77/(\beta_{\parallel i} + 0.016)^{0.76} = 0$, where the

numerical coefficients are chosen in order to fit the contour associated with the mirror instability growth rate $\gamma = 10^{-3}$ in unit of ion gyrofrequency, obtained in linear kinetic computations for bi-Maxwellian ions and isothermal electrons.

[22] Figure 3 (left) provides a color plot of the histogram of the numerical data in the plane ($\beta_{\|i}$, $T_{\perp i}/T_{\|i}$), in the case of a non-collisional FLR-Landau fluid simulation with β_0 = 0.6 and an energy threshold E_{M0}, after the mirror instability has developed and until $t = 10^5$, which compares to the time required for the slow wind to travel a distance of the order of 1 AU when Ω_i is of the order of a few tenths of second. In fact such long integrations are to be viewed as an artificial mean for the system to explore a large range of β. One observes that the data follow the above-defined threshold curve only during a limited time. As the simulation goes on, the temperature anisotropy tends to exceed the critical value. This behavior is consistent with the evolution of Γ in Figure 2, although the latter quantity retains the variation of the temperature of the electrons (which in our simulations are clearly non-isothermal).

[23] The agreement between the numerical data and the threshold curve extends to larger values of $\beta_{i\|}$ (not shown) when the threshold energy E_M is reduced. A much better agreement is obtained when collecting on the same graph the results of 9 different simulations with either $k_{\rm inj}r_L = 0.39$, or $k_{\rm inj}r_L = 0.55$, initialized with β_0 = 0.3, 0.6, 1.2 or β_0 = 0.6, 1.2, 2.4, 4.8, 7.2, 9.6 respectively, on a limited period of time (between 6000 and 25000 time units) following the development of the mirror instability (Figure 3, middle). This result indicates that although the model remains valid for increasing β, it develops, on long-time integrations, features that depart from solar wind observations.

[24] Long-time results remain significantly closer to the threshold curve when weak collisions are retained. Figure 3 (right) corresponds to simulations with collisions frequencies $\nu_{ie} = 10^{-5}$ (Figure 3, top right) and 0.25×10^{-5} (Figure 3, bottom right). We observe that during all the duration of the simulations, that extends up to 10^5 time units, the system remains confined in a close neighborhood of the threshold curve. At sufficiently small $\beta_{i\|}$, data lie now mostly below the theoretical curve, and no significant drift is observed when $\beta_{i\|}$ increases. These results suggest that deviations from bi-Maxwellianity are quite small in the regions of the slow solar wind sufficiently far from the sun, where the mirror instability is likely to develop. Although weak, collisions can contribute to this effect. A quantitative analysis would however require a more sophisticated collision model.

5. Conclusion

[25] The simulations presented in this paper show for the first time that a fluid model including low-frequency kinetic effects can address the problem of perpendicular heating in the solar wind conditions. It turns out that a low-frequency kinetic Alfvén wave turbulence can contribute to perpendicular ion heating and generate a self-regulated state where mirror instability limits further growth of temperature anisotropy. We demonstrate that although, in a collisionless regime, turbulence pushes the system beyond the mirror instability threshold, a small level of collisions is enough to balance this effect and constrain the system to follow the threshold curve in a ($\beta_\|$, $T_\perp/T_\|$) diagram, thus reproducing the behavior of measurements performed in the slow solar wind. Furthermore, the experimental determination of the temperatures, done by a fit of the data with an effective bi-Maxwellian distribution, does not depend greatly on the presence of wings in the distribution function (P. Hellinger, private communication, 2011). Since the mirror threshold is however sensitive to the presence of these wings, the good fitting of the border of the data points with the mirror instability threshold estimated in a bi-Maxwellian framework is an indication that large-velocity deviations from a bi-Maxwellian distribution are rather weak in the slow solar wind where the effect of collisions, although weak, is not fully negligible. We finally stress that this letter was concerned with dynamical processes taking place in the solar wind in regimes where the mirror instability is dominant. Further developments are required to analyze the competition between the instabilities in a turbulent regime, and also to take into account important other effects such as the expansion, needed to provide realistic temperature profiles.

[26] **Acknowledgments.** This work was supported in part by Programme Terre Soleil of INSU-CNRS. Part of the computations were performed on the Mesocentre SIGAMM machine hosted by the Observatoire de la Côte d'Azur.

[27] The Editor thanks an anonymous reviewer for assistance in evaluating this paper.

References

Alexandrova, O., J. Saur, C. Lacombe, A. Mangeney, J. Mitchell, J. Schwartz, and P. Robe (2009), Universality of solar-wind turbulent spectrum from MHD to electron scales, *Phys. Rev. Lett.*, *103*, 165003, doi:10.1103/PhysRevLett.103.165003.

Bale, S. D., J. C. Kasper, G. G. Howes, E. Quataert, C. Salem, and D. Sundkvist (2009), Magnetic fluctuation power near proton temperature anisotropy instability thresholds in the solar wind, *Phys. Rev. Lett.*, *103*, 211101, doi:10.1103/PhysRevLett.103.211101.

Bellan, P. M. (1994), Alfvén resonance reconsidered: Exact equations for wave propagation across a cold inhomogeneous plasma, *Phys. Plasmas*, *1*, 3523–3541.

Bhatnagar, P. L. (1962), On the BGK collision model for a two-component assembly, *Z. Astrophys.*, *54*, 234–243.

Borgogno, D., T. Passot, and P. L. Sulem (2007), Magnetic holes in plasmas close to mirror instability, *Nonlinear Processes Geophys.*, *14*, 373–383.

Bourouaine, S., E. Marsch, and F. M. Neubauer (2008), On the efficiency of nonresonant ion heating by corronal Alfvén waves, *Astrophys. J.*, *684*, L119–L122.

Brizard, A. J., and T. S. Hahm (2007), Foundations of nonlinear gyrokinetic theory, *Rev. Mod. Phys.*, *79*, 421–468.

Camporeale, E., T. Passot, and D. Burgess (2010), Implications of a non-modal theory for the marginal stability state and the dissipation of fluctuations in the solar wind, *Astrophys. J.*, *715*, 260–270.

Chandran, B. D. G., B. Li, B. L. Rogers, E. Quataert, and K. Germaschewski (2010), Perpendicular ion heating by low-frequency Alfvén-waves turbulence in the solar wind, *Astrophys. J.*, *720*, 502–515.

Green, J. M. (1973), Improved Bhatnagar-Gross-Krook model for electron-ion collisions, *Phys. Fluids*, *11*, 2022–2023.

Gross, E. P., and M. Krook (1956), Model for collision processes in gases: Small-amplitude oscillations of charged two-component systems, *Phys. Rev.*, *102*, 593–604.

Hellinger, P. (2007), Comment on the linear mirror instability near the threshold, *Phys. Plasmas*, *14*, 082105, doi:10.1063/1.2768318.

Hellinger, P., P. Trávníček, J. C. Kasper, and A. J. Lazarus (2006), Solar wind proton temperature anisotropy: Linear theory and WIND/SWE observations, *Geophys. Res. Lett.*, *33*, L09101, doi:10.1029/2006GL025925.

Livi, S., and E. Marsh (1986), Comparison of the Bhatnagat-Gross-Krook approximation with the exact Coulomb collision operator, *Phys. Rev. A*, *34*, 533–540.

Markovskii, S. A., B. J. Vasquez, and B. D. G. Chandran (2010), Perpendicular proton heating due to energy cascade of fast magnetosonic waves in the solar corona, *Astrophys. J.*, *709*, 1003–1008.

Matteini, L., S. Landi, P. Hellinger, F. Pantellini, M. Maksimovic, M. Velli, B. E. Goldstein, and E. Marsch (2007), Evolution of the solar wind proton temperature anisotropy from 0.3 to 2.5 AU, *Geophys. Res. Lett.*, *34*, L20105, doi:10.1029/2007GL030920.

Matteini, L., P. Hellinger, S. Landi, P. M. Trávníček, and M. Velli (2011), Ion kinetics in the solar wind: Coupling gloval expansion to local microphysics, *Space Sci. Rev.*, doi:10.1007/s11214-011-9774-z.
Pantellini, F. G. E., and S. J. Schwartz (1995), Electron temperature effects in the linear proton mirror instability, *J. Geophys. Res.*, *100*, 3539–3549.
Parashar, T. N., M. A. Shay, P. A. Cassak, and W. H. Matthaeus (2009), Kinetic dissipation and anisotropic heating in a turbulent collisionless plasma, *Phys. Plasmas*, *16*, 032310, doi:10.1063/1.3094062.
Passot, T., and P. L. Sulem (2007), Collisionless magnetohydrodynamics with gyrokinetic effects, *Phys. Plasmas*, *14*, 082502, doi:10.1063/1.2751601.
Pokhotelov, O. A., M. A. Balikhin, H. S.-C. K. Alleyne, and O. G. Onishchenko (2000), Mirror instability at finite electron temperature, *J. Geophys. Res.*, *105*, 2393–2401.
Price, C. P., D. W. Swift, and L.-C. Lee (1986), Numerical simulation of nonoscillatory mirror waves at the Earth's magnetosheath, *Geophys. Res. Lett.*, *91*, 101–112.
Schekochihin, A. A., S. C. Cowley, W. Dorland, G. W. Hammett, G. G. Howes, E. Quataert, and T. Tatsumo (2009), Astrophysical gyrokinetics: Kinetic and fluid turbulent cascades in magnetized weakly collisional plasmas, *Astrophys. J. Suppl.Ser.*, *182*, 310–377.
Snyder, P. B., G. W. Hammett, and W. Dorland (1997), Landau fluid models of collisionless magnetohydrodynamics, *Phys. Plasmas*, *4*, 3974–3985.
Štverák, Š., P. Trávníček, M. Maksimovic, E. Marsch, A. N. Fazakerley, and E. E. Scime (2008), Electron temperature anisotropy constraints in the solar wind, *J. Geophys. Res.*, *113*, A03103, doi:10.1029/2007JA012733.

D. Laveder, L. Marradi, T. Passot, and P. L. Sulem, Université de Nice-Sophia Antipolis, CNRS, Observatoire de la Côte d'Azur, BP 4229, F-06304 Nice CEDEX 4, France. (laveder@oca.eu; marradi@oca.eu; passot@oca.eu; sulem@oca.eu)